

Rayleigh Benard Convection of Bingham Fluid in A Square Enclosure with Sinusoidal Temperatures

Keddar Mohammed¹, Draoui Belkacem¹, Mebarki Brahim¹ and Medale Marc²

¹ Laboratory of Arid Zones Energetic - (ENERGARID), Faculty of Technology, University of Tahri Mohamed Bechar
BP 417 (08000), Bechar, Algeria

keddar.mohammed@univ-bechar.dz ; draoui.belkacem@univ-bechar.dz ;
brahim.mebarki@univ-bechar.dz

²Aix-Marseille University, Polytech Marseille, Energy Mechanics Dept IUSTI laboratory,
UMR 7343 CNRS-Aix-Marseille University Chateau-Gombert Technopole
5 rue Enrico Fermi 13453 MARSEILLE, Cedex 13, FRANCE

marc.medale@univ-amu.fr

Abstract - In this study, two-dimensional steady-state simulations of laminar natural convection of Rayleigh Benard in square enclosure were performed. The enclosure is considered to be completely filled with a yield stress fluid obeying visco-plastic model Bingham. The vertical lateral walls are thermally isolated, whereas sinusoidal temperature distributions with different amplitudes and phases are imposed over the horizontal walls. Fluid flow and heat transfer characteristics are systematically studied over a wide range of Rayleigh number Ra ($10^3 - 10^6$), and Bingham number Bn (0-20). We have fixed the Prandtl number ($Pr = 7$), Phase deviation $\phi = 0$ and finally amplitude ration $\varepsilon = 1$. The Navier-Stokes equations, the mass and energy conservation equations, are solved numerically using CFD software FLUENT. The results shows that the Nusselt number decreases with the increase of the Bingham number, and for the large values of the latter the heat transfer is done by conduction. It is also noteworthy that the increase in the phase difference and the amplitude ratio leads to the increase in the heat transfer.

Keywords: Natural convection, Convective flow, Non newtonian fluid, Viscoplastic fluid, Bingham fluid, Numerical simulation, Amplitude ratio, Phase deviation

1. Introduction

Viscoplastic fluids, defined by a yield stress τ_y , are known to exhibit a complicated transition between solid and fluid behaviour. If the material is not sufficiently strained, i.e. less than the yield stress, it does not flow and acts as a solid. It flows with shear-thinning behaviour above the yield stress. The inelastic Bingham [1], Herschel-Bulkley [2] and Casson [3] models are the most often employed for characterizing viscoplastic fluids. The Bingham model is the most basic approach for dealing with yield stress and it is the most commonly utilized model in theoretical and numerical investigations due to its relative simplicity. Natural convection in an enclosure [4-6] may be seen in various applications such as electronic equipment cooling, building cooling and heating, solar heaters, energy drying processes etc. Rayleigh-Bénard Convection (RBC) is a buoyancy-driven instability that occurs in a fluid layer heated from below and subjected to a temperature gradient. This arrangement occurs frequently in nature as well as in industrial processes, justifying the substantial amount of research committed to its comprehension. Refs [7-9] have been providing reviews for over a century, particularly in the case of Newtonian fluids. In comparison to the Newtonian case, the RBC in viscoplastic fluids has received less attention. However, interest in RBC in viscoplastic fluids has grown in recent decades, leading to theoretical and computational research [10-13]. There is also one of the most classic cases which is a differentially heated cavity filled with Bingham Fluids [14,15], where the vertical walls have different temperatures while the other walls (top and bottom) are adiabatic.

The present work aims to investigate a more complicated natural Rayleigh-Bénard convection in an enclosure with two sinusoidal temperature profiles on the top and the bottom walls, the enclosure is considered to be completely filled with a flow stress fluid obeying the Bingham model. The results indicate that the Nusselt number decreases with the increase of the Bingham number, and for the large values of the latter the heat transfer is done by conduction, also the increase in the phase difference and the amplitude ratio leads to the increase in the heat transfer.

2. Numerical methods

FLUENT, a commercial CFD software, provides the numerical model. Subject to the suggested boundary conditions, the conservation equations are discretized using a finite-volume technique based on the SIMPLEC algorithm. The second-order upwind differencing method is used to discretize the equations. Finally, the convergence requirements for solving the governing equations are regarded met when the sum of the residuals is less than 10^{-5} .

2.1. Geometry and boundary conditions

fig 1 presents the schematic diagram of the domain which the simulations will be run. Where thermal isolation exists between the vertical lateral walls, and the horizontal walls exhibit sinusoidal temperature distributions with varying amplitudes and phases. We make certain approximations and simplifying assumptions to reduce and simplify the mathematical formulation of the model and facilitate its resolution. Two-dimensional flow is assumed to be permanent; fluid flow is assumed to be incompressible and laminar, and finally thermo-physical properties of the fluid are constant, except for apparent viscosity, which varies according to the viscoplastic model, the Boussinesq approximation.

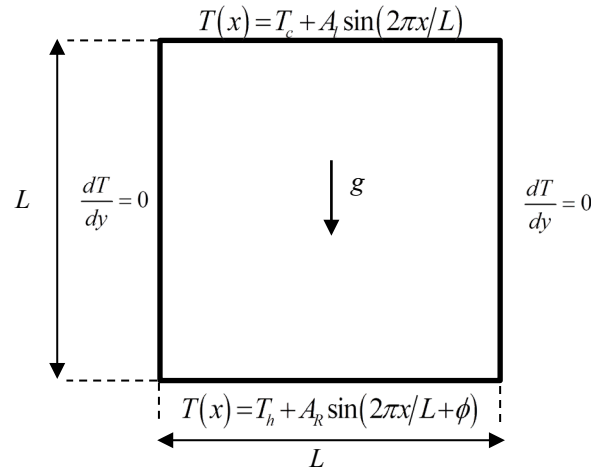


Fig. 1: Layout of the simulation domain.

2.2. Mathematical formulation

The steady-state conservation equations for mass, momentum, and energy in incompressible fluids are as follows. Continuity equation:

$$\frac{\partial u}{\partial x} + \frac{\partial v}{\partial y} = 0 \quad (1)$$

Momentum equations:

These equations are translated according to the Navier-Stokes equations.

Following x:

$$u \frac{\partial u}{\partial x} + v \frac{\partial u}{\partial y} = -\frac{\partial p}{\partial x} + \text{Pr} \left(2 \frac{\partial^2 u}{\partial x^2} + \frac{\partial^2 u}{\partial y^2} + \frac{\partial^2 v}{\partial x \partial y} \right) + \left(2 \frac{\partial \mu_a}{\partial x} \frac{\partial u}{\partial x} + \frac{\partial \mu_a}{\partial y} \frac{\partial u}{\partial y} + \frac{\partial \mu_a}{\partial y} \frac{\partial v}{\partial x} \right) \quad (2)$$

Following y:

$$u \frac{\partial v}{\partial x} + v \frac{\partial v}{\partial y} = -\frac{\partial p}{\partial y} + \text{Pr} \left(2 \frac{\partial^2 v}{\partial y^2} + \frac{\partial^2 v}{\partial y^2} + \frac{\partial^2 u}{\partial x \partial y} \right) + \left(\frac{\partial \mu_a}{\partial x} \frac{\partial u}{\partial x} + 2 \frac{\partial \mu_a}{\partial y} \frac{\partial v}{\partial y} + \frac{\partial \mu_a}{\partial x} \frac{\partial u}{\partial y} \right) + Ra \text{Pr} \theta \quad (3)$$

The energy equation:

$$u \frac{\partial \theta}{\partial x} + v \frac{\partial \theta}{\partial y} = \left(\frac{\partial^2 \theta}{\partial x^2} + \frac{\partial^2 \theta}{\partial y^2} \right) \quad (4)$$

These variables have been used to make the above equations dimensionless

$$x = \frac{x^*}{L}, \quad y = \frac{y^*}{L}, \quad u = \frac{u^* L}{\alpha}, \quad v = \frac{v^* L}{\alpha}, \quad p = \frac{p^* L}{\rho \alpha^2}, \quad \theta = \frac{T - T_c}{T_h - T_c}$$

The Bingham model is governed by the following equations:

$$\begin{cases} \dot{\gamma} = 0 & \text{if } \tau \leq \tau_0 \\ \tau = \left(\mu + \frac{\tau_0}{\dot{\gamma}} \right) \dot{\gamma} & \text{if } \tau > \tau_0 \end{cases} \quad (5)$$

Dimensionless Rayleigh number:

$$Ra = \frac{\rho^2 C_p g \beta \Delta T L^3}{\mu \lambda} = Gr \text{Pr} \quad (6)$$

Dimensionless Grashoff number:

$$Gr = \frac{\rho^2 g \beta \Delta T L^3}{\mu^2} \quad (7)$$

Dimensionless Prandtl number:

$$\text{Pr} = \frac{\mu C_p}{\lambda} \quad (8)$$

Dimensionless Bingham number:

$$Bn = \frac{\tau_0}{\mu} \sqrt{\frac{L}{g \beta \Delta T L}} \quad (9)$$

Boundary conditions are as follows:

At the top $u = v = 0, \theta = \sin(2\pi x)$

At the bottom of the domain $u = v = 0, \theta = \varepsilon \sin(2\pi x + \phi)$

The vertical walls $u = v = 0, \frac{dT}{dy} = 0$

Where $\varepsilon = AR / AI$ is the amplitude of the sinusoidal temperature which is at the bottom and at the top of the cavity, with AR being the aspect ratio and $AR = H / L$ et $AI = T_h - T_c$

2.3 Validation

To validate our results, we compared them with those of the literature, namely the work of references [4] and [13]. A good agreement has been noted between our numerical results and those of the articles [4] and [13].

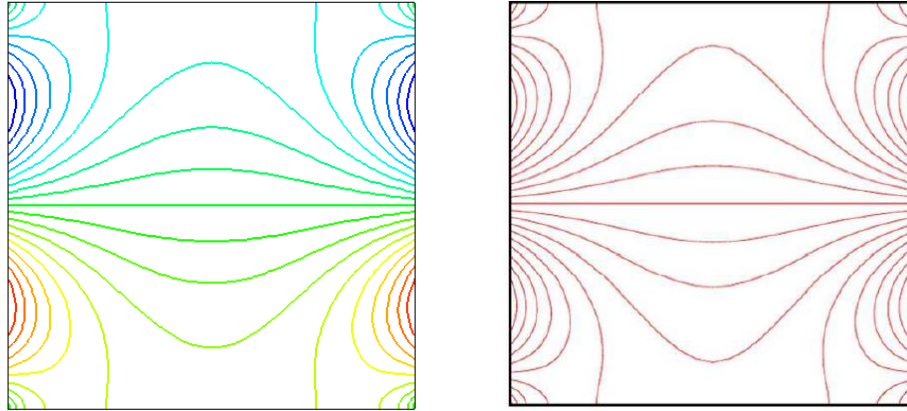


Fig 2: Comparison of numerical result obtained (left) with [4] (right) of the Effect of Rayleigh number on the isotherms at $Ra = 10^3$, $Bn = 0$, $Pr = 0.7$, $\phi = 0$ and $\varepsilon = 1$.

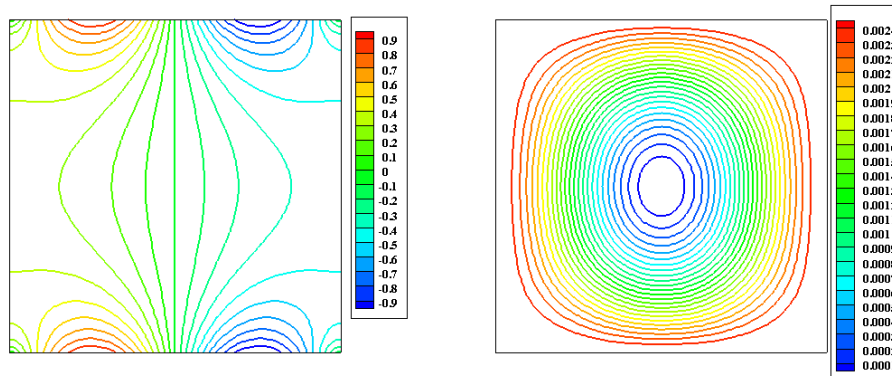
Table 1: Nusselt validation [13]

	$Bn = 1$	$Bn = 3$	$Bn = 6$	$Bn = 9$	$Bn = 18$	$Bn = 27$
$Ra = 10^5$						
Huilgol [13]	3.303	3.263	3.083	2.898	2.402	2.143
Present work	3.305	3.265	3.083	2.900	2.403	2.140

3 Results and discussion

3.1 Effect of Rayleigh number

At low Rayleigh number, $Ra = 10^3$, convection is very weak and therefore heat transfer is dominated by the mechanism of conduction, as shown by the isotherms. As the Rayleigh number increases up to $Ra = 10^5$, the structure of the isotherms as well as the streamlines start to change for Bingham fluid as seen in Fig 3. We observe that the streamlines are in the form of one cell, but the shape of this cell changes and deforms with the increase of the Rayleigh number. Obviously, at this point, triggers convection.



(a) : $Ra = 10^3$

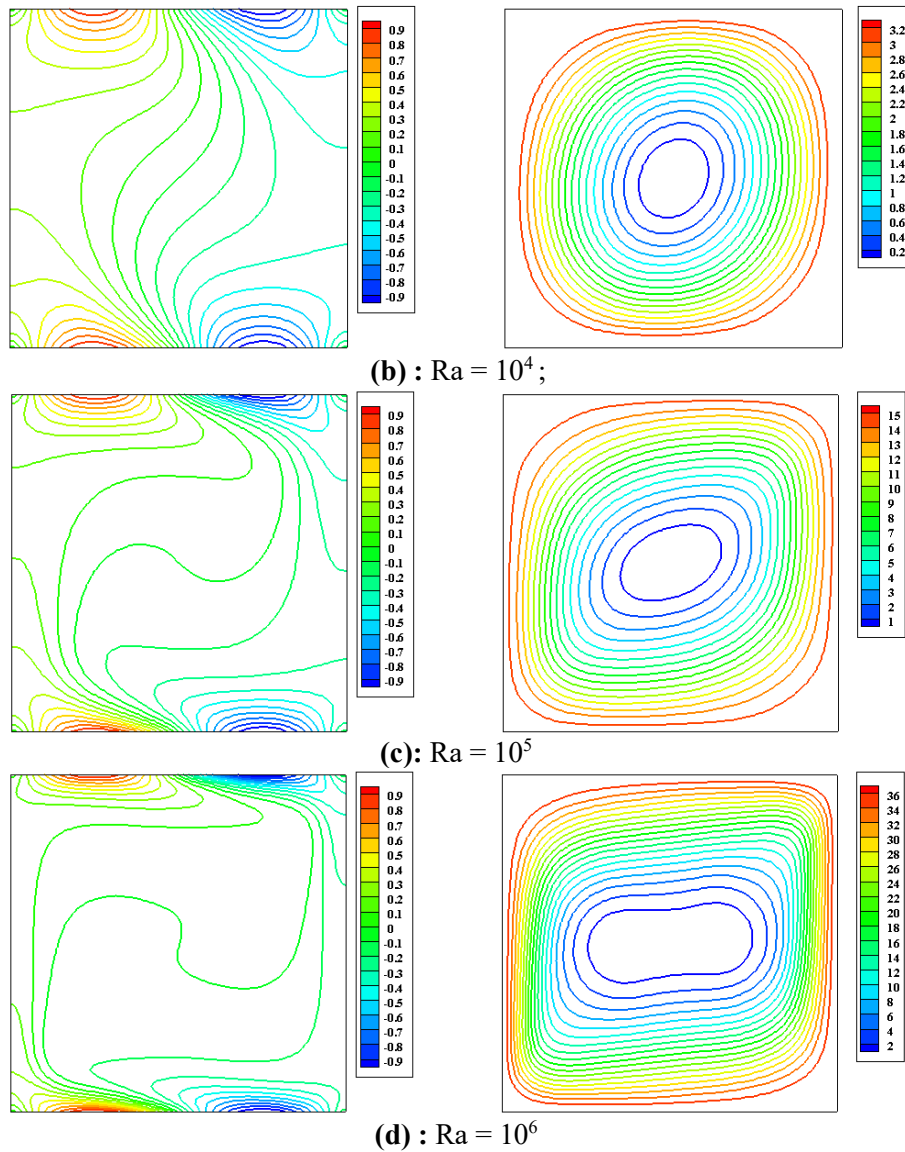
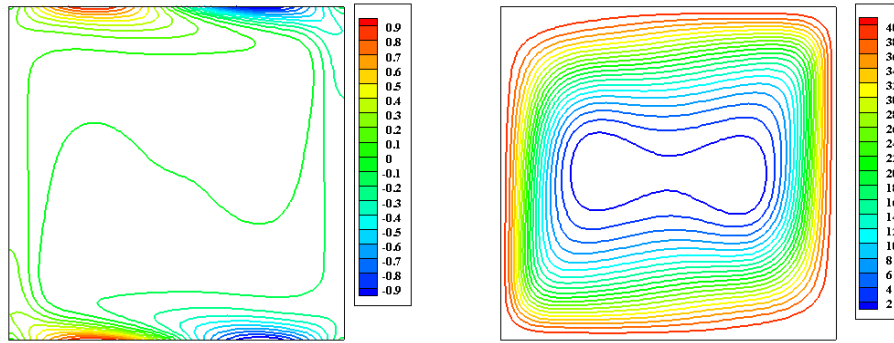


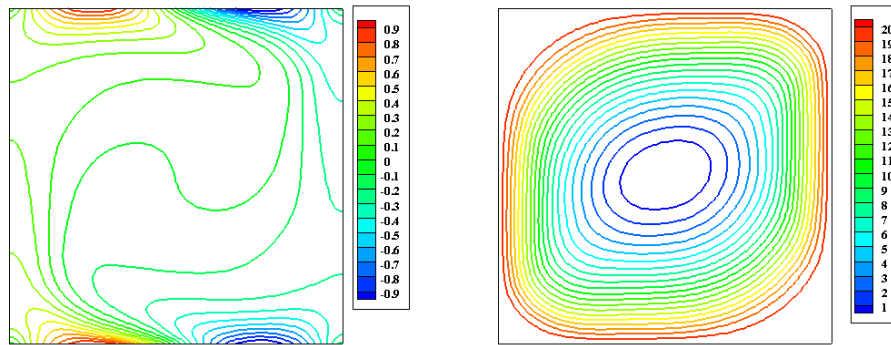
Fig 3 : Contours of isotherms (left) and streamlines (right) of the Bingham fluid for $Bn = 0,5$; $Pr = 7$; $\phi = 0$; $\varepsilon = 1$.

3.2 Effect of Bingham number

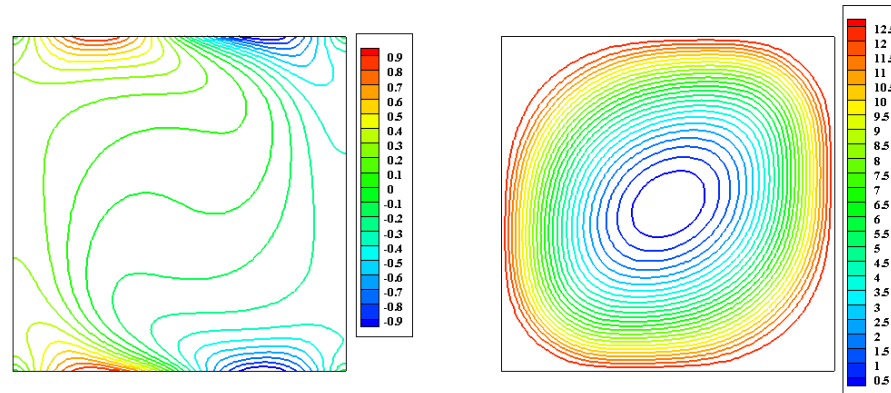
For high values of the Bingham number, the viscous force more easily overcomes the buoyant force and therefore no flux is induced inside the enclosure. This behaviour can be better understood by comparing the contours of the streamlines and non-dimensional isotherms shown in Fig 4 for different values of Bn at $Ra=10^6$. These figures suggest that the effects of convection inside the enclosure decrease with increasing Bn and as the Bingham fluid begins to behave like a solid, the fluid velocities drop to values so low that for all intents and purposes, the fluid is essentially stagnant. In the absence of flux in the enclosure, heat transfer takes place by conduction.



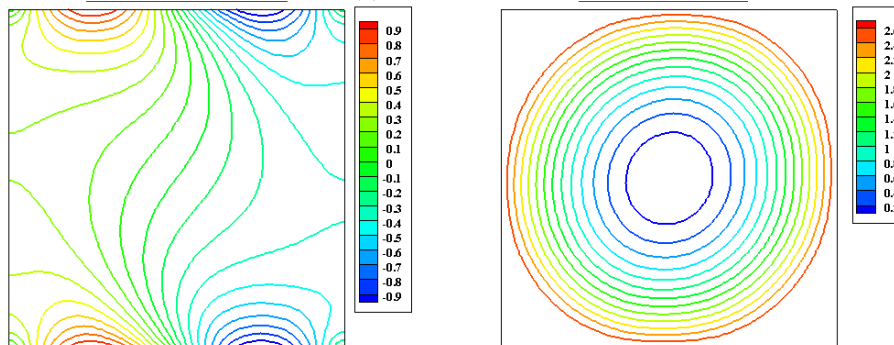
(a): $Ra = 10^6$; $Bn = 0$



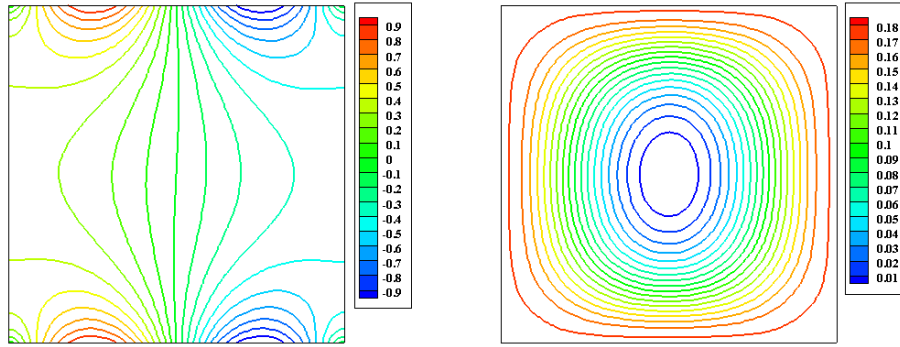
(b): $Ra = 10^6$; $Bn = 3$



(c): $Ra = 10^6$; $Bn = 5$



(d): $Ra = 10^6$; $Bn = 10$



(f): $Ra = 10^6$; $Bn = 20$
Fig 4 : Contours of isotherms (left) and streamlines (right) of the Bingham fluid for $Pr = 7$; $\phi = 0$; $\varepsilon = 1$.

3.3 Heat transfer quantification

The variation of Nusselt number is shown in fig 5 . The results reveal that the Nusselt number drops as the Bingham number increases, and that for large values of the latter, heat transmission occurs by conduction. It is also worth noting that increasing the phase difference and amplitude ratio increases heat transmission.

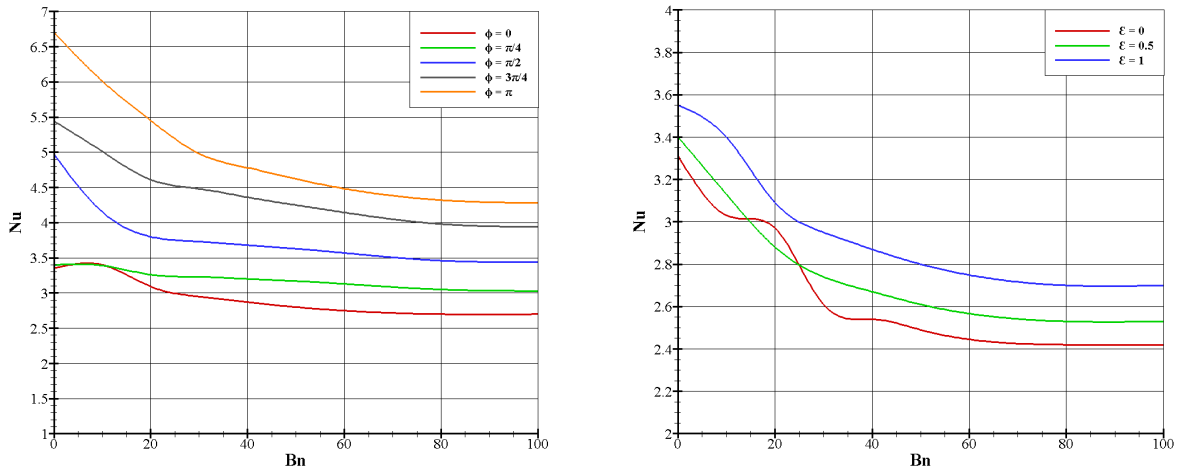


Fig 5: Effect of the phase deviation (ϕ) and the amplitude ratio (ε) on the average Nusselt for $Ra = 10^6$, $Pr = 0.1$ $\phi = 0$ and $\varepsilon = 1$ respectively

4 Conclusion

This work concerns a numerical study of the two-dimensional natural Rayleigh benard convection of a non-Newtonian viscoplastic fluid. The viscoplastic behaviour is described by the Bingham model. The two-dimensional convective flow considered is confined in a cavity, where vertical walls are thermally insulated and the horizontal walls have two sinusoidal temperatures. The Navier-Stokes equations, the mass and energy conservation equations, are solved numerically using an industrial numerical simulation code CFD: FLUENT.

- The Nusselt number decreases with the increase of the Bingham number, and for the large values of the latter the heat transfer is done by conduction.

- The increase in the phase difference leads to the increase in the heat transfer, with regard to the influence of the phase deviation on the Nusselt. It is observed that from the values, the heat transfer rate is improved for $\phi = \pi$.
- Heat transfer increases as the amplitude ratio increases. The heat transfer rate for $\varepsilon = 1$ is higher than in the other cases.

5 References

- [1] E. Bingham. The behavior of plastic materials, Bull US Bur Stand 13 (1916) 309–353.
- [2] W.H. Herschel, R. Bulkley, Measurement of consistency as applied to rubber-benzene solutions, Am Soc Test Proc 26 (2) (1926).
- [3] Aneja, M., Chandra, A., & Sharma, S. (2020). Natural convection in a partially heated porous cavity to Casson fluid. *International Communications in Heat and Mass Transfer*, 114, 104555.
- [4] Deng H.Q., Chang. J.J. (2008). Natural convection in a rectangular enclosure with sinusoidal temperature distributions on both side walls, *Numerical Heat Transfer, Part A*, Vol. 54, pp. 507-524.
- [5] A. Bejan. Convective Heat Transfer, Wiley New York, 1984,
- [6] G. de Vahl Davis, Natural convection of air in a square cavity: a bench mark numerical solution, Int. J. Numer. Methods Fluids 3 (1983) 249–264.
- [7] S. Chandrasekhar, Hydrodynamic and hydromagnetic stability, Clarendon, Oxford, 1961.
- [8] E.L. Koschmieder, Bénard cells and Taylor vortices, Cambridge University Press, 1993.
- [9] E. Bodenschatz, W. Pesch, G. Ahlers, Recent developments in Rayleigh-Bénard convection, Annu Rev Fluid Mech 32 (1) (Jan. 2000) 709–778.
- [10] Aghighi, M. S., Ammar, A., Metivier, C., & Gharagozlu, M. (2018). Rayleigh-Bénard convection of Casson fluids. *International Journal of Thermal Sciences*, 127(February 2017), 79–90.
- [11] Sun, M. H., Wang, G. B., & Zhang, X. R. (2019). Rayleigh-Bénard convection of non-Newtonian nanofluids considering Brownian motion and thermophoresis. *International Journal of Thermal Sciences*, 139(February), 312–325.
- [12] Yigit, S., Hasslberger, J., Chakraborty, N., & Klein, M. (2020). Effects of Rayleigh-Bénard convection on spectra of viscoplastic fluids. *International Journal of Heat and Mass Transfer*, 147, 118947.
- [13] Huilgol, R. R., & Kefayati, G. H. R. (2015). Natural convection problem in a Bingham fluid using the operator splitting method. *Journal of Non-Newtonian Fluid Mechanics*, 220, 22–32.
- [14] Turan, O., Chakraborty, N., & Poole, R. J. (2010). Laminar natural convection of Bingham fluids in a square enclosure with differentially heated side walls. *Journal of Non-Newtonian Fluid Mechanics*, 165(15–16), 901–913.